XL CILAMCE
IBERO-LATIN AMERICAN CONGRESS ON COMPUTATIONAL METHODS IN ENGINEERING
NOVEMBER 11-14, 2019
Praiamar Natal Hotel & Convention
Natal, RN-BRAZIL

FINITE ELEMENT METHOD APPLIED TO HIGHER-ORDER ZIG-ZAG THEORY FOR LAMINATED BEAMS

Hilton M. S. Santana
Fabio C. da Rocha
hiltonmarquess@gmail.com
fcrocha@ufs.br
Federal University of Sergipe
Marechal Randon Avenue s/n, 49400-00, São Cristovão/Sergipe, Brazil
Maria S. M. Sampaio
socorrosampaio@hotmail.com
Lutheran University of Brazil – CEULM/ULBRA
Carlos Drummond de Andrade Avenue 1460, Atílio Andreazza, 69077-730, Manaus/Amazonas, Brazil

Abstract. Due to the continuing importance of laminated materials in civil, naval, mechanical and aerospace engineering, the development of structural analysis theories of laminated beams has been an active area of research. The well-known classical theories of Euler-Bernoulli and Timoshenko have limitations because they do not present a field of shear deformation or by the incorrect consideration of such deformations, without respecting the nullity of the shear stress in the edges of the beam. Thus, high-order theories have emerged to remedy the limitations of classical theories, especially the Equivalent Single Layer (ESL) theories. In ESL theory, the displacement function in the thickness coordinate are assumed to Class C^1. This feature provides a discontinuous shear stress field at the interfaces of adjacent layers with different materials. In the 1980s, DiSciuva introduced a new class of laminated theories, where a zig-zag function is added to the ESL theories to describe the displacement in the thickness coordinate. This new theory allows the continuity of interlaminar tensions and a number of variables independent of the number of layers of the beam. In this way, the present work seeks to present the complete development of a finite element model of several ESL-Zig-Zag theories. Thus, a unified displacement field will be used that allows the simultaneous development and comparison of several refined theories found in the literature. After obtaining the governing equations, the finite element model is constructed using the Lagrange and Hermite polynomial functions. Finally, to show the good efficiency of the finite element model, numerical results are shown and compared with the exact solution of the elasticity of Pagano (1970).

Keywords: Laminated beams, ESL theories, Finite Element Method, Higher-Order Zig-Zag Theory

1 INTRODUCTION

In recent decades, composite beams have come to play a primary role in civil, mechanical, aeronautical and robotic engineering applications. As a result, the need for theories that could effectively describe the mechanical behavior of a laminated composite beam also increased. The classical Euler-Bernoulli (EBT) theory, although widely known, fails in considering the null shear strain and the cross section of the beam remains flat and orthogonal to the neutral line after deflexion. Thus, at the beginning of the twentieth century, Timoshenko [1] proposes a First Order Theory (FOT) that considers constant shear strain along the cross section. However, because it does not consider the possibility of shear stress nullity at the beam edges, FOT needs correction factors for an improvement in its efficiency. From the middle of the twentieth century, high order theories have come to describe the shear strain of the beam without the need for correction factors ([2-9]). The high order theories propose for their displacement field, polynomial, trigonometric or exponential functions that allow the nullity of shear stress at the edges of the beam without incurring the need for correction factors. These theories were initially proposed for the analysis of isotropic and homogeneous beams. However, it is possible to extend its use to the analysis of orthopedic and laminated beams through three types of theories commonly found in the literature: Equivalent Layer Theories (ELT), Layerwise Theories (LW) and Zig-Zag Theories (ZZ).

ELT, LW and ZZ theories differ mainly in the number of variables found in the differential equation system and in the possibility of zigzag behavior along the beam cross section. The ELT theory (Sayyad et al [10]), while simpler, has the disadvantage of assuming a C^1 displacement field that results in a continuous strain field and since the layers have different transverse shear modulus, the shear stress field will be discontinuous. The LW theory (Reddy [11]) proposes the construction of an independent displacement field for each beam layer, however, the amount of variables will increase proportionally with the number of layers, which considerably increases the computational cost of the theory (in practical applications it is common for the number of layers to exceed 100). In the 1980s, DiSciuva [12] proposed a displacement field in which a piecewise function allows zigzag behavior, so the number of variables remains independent of the number of beam layers. In order to improve the efficiency of this theory for the clamped boundary and enable its implementation by finite element method with C^0 functions, it was proposed in DiSciuva et al [13] the Refined ZigZag Theory (RZZ). Thus, among the mentioned theories, the RZZ theory presents the ideal combination of efficiency and cost computational.

In this paper, several high order models are developed simultaneously in conjunction with the ZZ theory for the analysis of the static and dynamic behavior of symmetrical and asymmetric laminated beams subjected to a transversal loading. The equations that describe the problem are derived from the Hamilton principle. A C^1 finite element model using interdependent interpolation functions is also developed. The numerical results are compared with the elasticity theory obtained in Pagano [14] and Giunta et al. [15]

2 GOVERNING EQUATIONS

2.1 Kinematics

Consider a beam of thickness *h*, composed of *N* orthotropic layers with the main material coordinates (x_1^k, x_x^k, x_3^k) of the *kth* layer oriented at an angle θ_k related to the x coordinate. The *kth* layer is located between the points $z = z_k$ and $z = z_{k+1}$ in the thickness direction (Fig. 1).

In order to cover the kinematics of various refined theories, the unified field of displacement given in Eq. (1) is used:

$$\begin{cases} u(x,z,t) = u_o - z\dfrac{\partial w}{\partial x} + f(z)\phi + \displaystyle\sum_{k=1}^{N-1} \psi_k(z - z_k)Y, \\ w(x,z,t) = w(x,t), \end{cases} \tag{1}$$

where, $u(x,z,t), u_o(x,t), w(x,t)$ and $\phi(x,t)$ represent, respectively, the axial displacement, the axial displacement of the centroidal axis, the transverse displacement of the centroidal axis and the cross section rotation due to shear, z_k is the *z* coordinate at the *N-1* beam interface, $\psi_k(x,t)$ is an unknown function and *Y* is a singular function worth 1 when $\left(z - z_k\right) \geq 0$ and worth *0* when $\left(z - z_k\right) < 0$ and $f(z)$ is a function that describes the used shear theory as shown in Table 1.

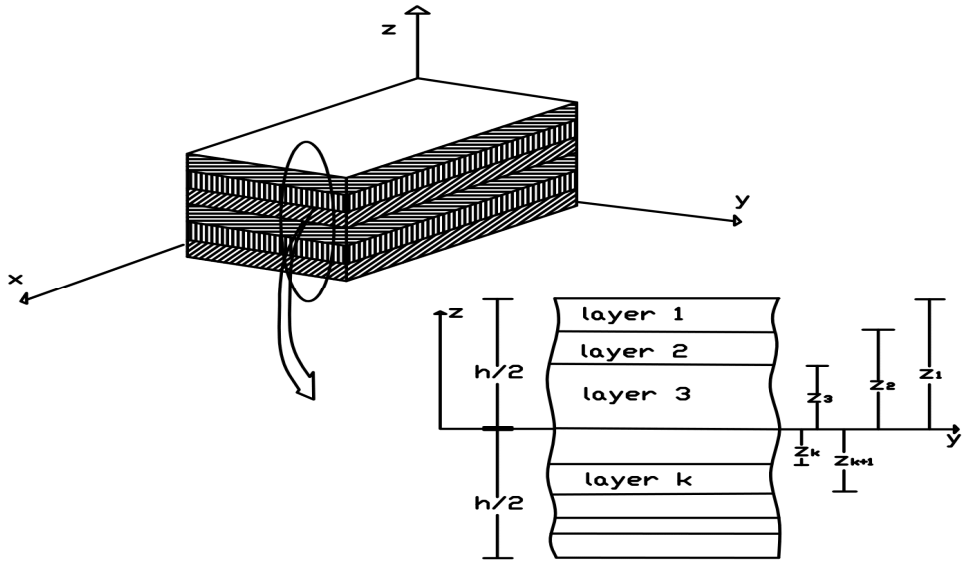

Figure 1. Laminate composite beam geometry.

The adopted strain field is presented in Eqs. 2(a and b):

$$\varepsilon_{xx} = \frac{\partial u}{\partial x} = \frac{\partial u_o}{\partial x} - z\frac{\partial^2 w}{\partial x^2} + f(z)\frac{\partial \phi}{\partial x} + \sum_{k=1}^{N-1}\frac{\partial \psi_k}{\partial x}\left(z - z_k\right)Y \ , \tag{2a}$$

$$\gamma_{xz} = \left(\frac{\partial w}{\partial x} + \frac{\partial u}{\partial z}\right) = \frac{df(z)}{dz}\left(\phi\right) + \sum_{k=1}^{N-1}\psi_k Y \, . \tag{2b}$$

Using the constitutive law for ortotropic materials (Reddy [11]), the stress field in Eqs. 3(a and b) can be achieved:

$$\sigma_{xx} = Q_{11}\varepsilon_{xx} \, , \tag{3a}$$

$$\tau_{xz} = Q_{55}\gamma_{xz} \, , \tag{3b}$$

where:

$$Q_{11} = \frac{1}{(-1 + v_{xy}v_{yx})}\begin{Bmatrix} E_{xx}cos(\theta)^4 + (E_{yy}v_{xy} + E_{xx}v_{yx})cos(\theta)^2 sin(\theta)^2 + E_{yy}sin[\theta]^4 + \\ G_{xy}(1 - v_{xy}v_{yx})sin[2\theta]^2 \end{Bmatrix}, \tag{4}$$

$$Q_{55} = G_{zx}\cos(\theta)^2 + G_{yz}\sin(\theta)^2 \, . \tag{5}$$

In Eqs. (4 and 5), $E_{ii,}$ and G_{ij} *(i=x,y)* are, respectively, the Young and the Shear modules in relation to the main axes; θ is the angle that the fiber makes with the main axis of the beam.

To ensure the continuity of shear stress, the following condition is imposed:

$$\lim_{z\to z_i} \tau_{xz}^{(k+1)} = \lim_{z\to z_i} \tau_{xz}^{(k)} . \tag{6}$$

Table 1. Shear theory used in the displacement field.

Model	Author	Function $f(z)$
Model 1	Reddy [2]	$f(z)=\left[\frac{z}{2}\left(\frac{h^2}{4}-\frac{z^2}{3}\right)\right]$
Model 2	Shi –Voyiadjis [3]	$f(z)=\left[\frac{5z}{4}\left(1-\frac{4z^2}{3h^2}\right)\right]$
Model 3	Ambartsumyan [4]	$f(z)=z\left[1-\frac{4z^2}{3h^2}\right]$
Model 4	Touratier [5]	$f(z)=\frac{h}{\pi}\sin\left[\frac{\pi z}{h}\right]$
Model 5	Soldatos [6]	$f(z)=\left[z\cosh\left(\frac{1}{2}\right)-h\sinh\left(\frac{z}{h}\right)\right]$
Model 6	Karama et al. [7]	$f(z)=z\exp\left[-2\left(\frac{z}{h}\right)^2\right]$
Model 7	Akavci [8]	$f(z)=\frac{3\pi}{2}\left[h\tanh\left(\frac{z}{h}\right)+ -z\sec^2\left(\frac{1}{2}\right)\right]$
Model 8	Thai et al. [9]	$f(z)=h\tan^{-1}\left(\frac{2z}{h}\right)-z$

After replacing Eq. (3b) in Eq.(6), results:

$$\psi_k = \phi^{ZZ} a_k , \tag{7}$$

where:

$$a_k = \left(\frac{Q_{55}^k - Q_{55}^{k+1}}{Q_{55}^{k+1}}\right)\left(f'(z_k)+\sum_{q=1}^{k-1} a_q\right). \tag{8}$$

The Hamilton principle (Reddy [16]) is used to obtain the equations of motion for the displacement field given in Eq. (1). Thus, the equations that describe the theory are presented in Eq. 9 (a, b and c):

$$-\frac{\partial^2 N_x}{\partial x^2}+\frac{\partial R_0}{\partial t}=0 . \tag{9a}$$

$$\frac{\partial^3 M_x}{\partial x^3}+\frac{\partial R_2}{\partial x\partial t}+\rho b h\frac{\partial^2 w}{\partial t^2}=q . \tag{9b}$$

$$-\frac{\partial^2 P_x}{\partial x^2}-\frac{\partial^2 M_x^a}{\partial^2 x}+R_x+T_x^a+\frac{\partial S_0}{\partial t}+\frac{\partial T_0}{\partial t}=0 . \tag{9c}$$

where:

$$N_x = A_0 u_o - B_0 \frac{\partial w}{\partial x} + (D_0 + G_0)\phi, \quad R_0 = \frac{\rho}{Q_{11}^k}\frac{\partial N_x}{\partial t}, k = 1,2...N\,. \tag{10a}$$

$$M_x = -B_0 u_o + C_0 \frac{\partial w}{\partial x} - (E_0 + H_0)\phi, \quad R_2 = \frac{\rho}{Q_{11}^k}\left(\frac{\partial M_x}{\partial t}\right), k = 1,2...N\,. \tag{10b}$$

$$P_x = (D_0)u_o - (E_0)\frac{\partial w}{\partial x} + (F_0 + I_0)\phi, \quad S_0 = \frac{\rho}{Q_{11}^k}\left(\frac{\partial P_x}{\partial t}\right), k = 1,2...N\,. \tag{10c}$$

$$M_x^a = (G_0)u_o - (H_0)\frac{\partial w}{\partial x} + (I_0 + J_0)\phi, \quad T_0 = \frac{\rho}{Q_{11}^k}\left(\frac{\partial M_x^a}{\partial t}\right), k = 1,2...N\,. \tag{10d}$$

$$R_x = (K_0 + L_0)\phi, \quad T_x^a = (L_0 + M_0)\phi\,. \tag{10e}$$

$$\left[A_0, B_0, C_0\right] = \sum_{k=1}^{N}\int_{z_{k+1}}^{z_k}(1, z, z^2) b Q_{11}^k dz\,. \tag{10f}$$

$$\left[D_0, E_0, F_0\right] = \sum_{k=1}^{N}\int_{z_{k+1}}^{z_k}\left[1, z, f(z)\right] f(z) b Q_{11}^k dz\,. \tag{10q}$$

$$\left[G_0, H_0, I_0, J_0\right] = \sum_{k=1}^{N}\int_{z_{k+1}}^{z_k}\left[1, z, f(z), \sum_{k=1}^{N-1} a_k\left(z - z_k\right)Y\right]\sum_{k=1}^{N-1} a_k\left(z - z_k\right) Y b Q_{11}^k dz\,. \tag{10h}$$

$$\left[K_0, L_0\right] = \sum_{k=1}^{N}\int_{z_{k+1}}^{z_k}\left[f'(z), \sum_{k=1}^{N-1} a_k Y\right] f'(z) b Q_{55}^k dz, \quad M_0 = \sum_{k=1}^{N}\int_{z_{k+1}}^{z_k}\left(\sum_{k=1}^{N-1} a_k Y\right)^2 b Q_{55}^k dz\,. \tag{10i}$$

where b, h, N, ρ and q represent, respectively, the section width, its height, the numbers of layers present in the laminated beam, its density and the applied distributed loading. In addition to the domain equations (Eqs. 9a-c and 10a-i), we have the following boundary conditions:

$$\begin{Bmatrix} w \\ \dfrac{\partial w}{\partial x} \\ \phi \\ u_o \end{Bmatrix} \quad \text{or} \quad \begin{Bmatrix} \hat{V}_x = -\dfrac{\partial^2 M_x}{\partial x^2} - \dfrac{\partial R_2}{\partial x} \\ \widehat{M}_{xx} = \dfrac{\partial M_x}{\partial x} \\ \overline{M} = \dfrac{\partial P_x}{\partial x} + \dfrac{\partial M_x^a}{\partial x} \\ \widehat{N} = \dfrac{\partial N_x}{\partial x} \end{Bmatrix}. \tag{11}$$

For dynamic purposes Eqs. (9a-c) can be formulated considering an eigenvalue problem to find natural frequencies. Thus, Eqs. (12a-c) represent the periodic movement of the beam under free vibration (Reddy [17]):

$$u_o(x,t) = U(x)e^{-i\omega t}\,. \tag{12a}$$

$$w(x,t) = W(x)e^{-i\omega t}\,. \tag{12b}$$

$$\phi(x,t) = S(x)e^{-i\omega t}. \tag{12c}$$

where ω is the natural frequency of transverse motion, $U\left(x\right)$,$W\left(x\right)$ and $S\left(x\right)$ are the modal shape of the transverse motion. Replacing Eqs. (12 a-c) in Eqs. (9 a-c) (being $q=0$) gives an eigenvalue problem whose solution represents the natural frequency of the beam subjected to free vibration.

2.2 Shear stress

Although the shear stress field of the present theory is continuous, it is possible to refine the results by employing the methodology for obtaining the shear stress given by Reddy [11]. Reddy [11] proposed an alternative way to obtain interlaminar stresses through the equilibrium equations of three-dimensional elasticity:

$$\begin{aligned} 0 &= \frac{\partial \sigma_{xx}}{\partial x} + \frac{\partial \tau_{xy}}{\partial y} + \frac{\partial \tau_{xz}}{\partial z}, \\ 0 &= \frac{\partial \tau_{yx}}{\partial x} + \frac{\partial \sigma_{yy}}{\partial y} + \frac{\partial \tau_{yz}}{\partial z}, \\ 0 &= \frac{\partial \tau_{zx}}{\partial x} + \frac{\partial \tau_{zy}}{\partial y} + \frac{\partial \sigma_{zz}}{\partial z}. \end{aligned} \tag{13}$$

For each layer, Eqs. (13) can be integrated with respect to *z* and obtain interlaminar stresses within each layer ($z_k \le z \le z_{k+1}$). Thus, the shear stress τ_{xz} is given as:

$$\tau_{xz} = -\int_{z_k}^{z} \left(\frac{\partial \sigma_{xx}}{\partial x} + \frac{\partial \tau_{xy}}{\partial y} \right) dz + G^{(k)}, \tag{14}$$

where $G^{(k)}$ is an integration constant that can be obtained through the nullity of shear stress at the beam edges and the interlaminar continuity condition.

3 FINITE ELEMENT MODEL

This section discusses the development of the finite element method applied to the ZZ theory for laminated beams. In this paper, the Hermite cubic approximation is used for both, the deflection and its derivative, and the Lagrange quadratic approximation for the variables $u_o(x,t)$ and $\phi(x,t)$, in order to avoid the shear locking effect (Reddy [16]).

3.1 FEM formulation for the theory

For the Higher-Order Zig-Zag FEM formulation (FEM-ZZ), aproximations for the $w(x,t)$, $u_0\left(x,t\right)$ and $\phi\left(x,t\right)$ are considered as follows:

$$w(x,t) \approx \sum_{i=1}^{m} w_i(t)\varphi_i^{(1)}(x), \quad u_o(x,t) \approx \sum_{j=1}^{n} u_j(t)\varphi_j^{(2)}(x), \quad \phi(x,t) \approx \sum_{j=1}^{n} \phi_j(t)\varphi_j^{(2)}(x), \tag{15}$$

where $\varphi_j^{(1)}$ and $\varphi_j^{(2)}$ are Hermite cubic and Lagrange quadratic polynomial interpolation functions, respectively, w_i are nodal values consisting of $w\left(x,t\right)$, u_j are nodal values consisting of $u_o\left(x,t\right)$ and

ϕ_j are nodal values consisting of $\phi(x,t)$. Replacing Eq. 15 in the weak formulation of Eqs. 9(a-c) gives the following finite element model:

$$\begin{bmatrix} [K^{11}] & [K^{12}] & [K^{13}] \\ [K^{21}] & [K^{22}] & [K^{23}] \\ [K^{31}] & [K^{32}] & [K^{33}] \end{bmatrix} \begin{Bmatrix} \{w\} \\ \{\phi\} \\ \{u\} \end{Bmatrix} + \begin{bmatrix} [M^{11}] & [M^{12}] & [M^{13}] \\ [M^{21}] & [M^{22}] & [M^{23}] \\ [M^{31}] & [M^{32}] & [M^{33}] \end{bmatrix} \begin{Bmatrix} \{\ddot{w}\} \\ \{\ddot{\phi}\} \\ \{\ddot{u}\} \end{Bmatrix} = \begin{Bmatrix} \{F^1\} \\ \{F^2\} \\ \{F^3\} \end{Bmatrix}, \tag{16}$$

where:

$$\begin{aligned}
K_{ii}^{11} &= \int_{x_a}^{x_b} \left(C_0 \frac{d^2\varphi_i^{(1)}}{dx^2} \frac{d^2\varphi_i^{(1)}}{dx^2} \right) dx, & K_{ij}^{12} &= \int_{x_a}^{x_b} \left(-\left(E_0 + H_0\right) \frac{d^2\varphi_i^{(1)}}{dx^2} \frac{d\varphi_j^{(2)}}{dx} \right) dx, \\
K_{ji}^{21} &= \int_{x_a}^{x_b} \left(-\left(E_0 + H_0\right) \frac{d\varphi_j^{(2)}}{dx} \frac{d^2\varphi_i^{(1)}}{dx^2} \right) dx, & K_{jj}^{22} &= \int_{x_a}^{x_b} \left(\begin{matrix} (F_0 + 2I_0 + J_0) \frac{d\varphi_j^{(2)}}{dx} \frac{d\varphi_j^{(2)}}{dx} + \\ \left(K_0 + 2L_0 + M_0\right) D_0 \varphi_j^{(2)} \varphi_j^{(2)} \end{matrix} \right) dx, \\
K_{ij}^{13} &= \int_{x_a}^{x_b} \left(-\left(B_0\right) \frac{d^2\varphi_i^{(1)}}{dx^2} \frac{d\varphi_j^{(2)}}{dx} \right) dx, & K_{ji}^{31} &= \int_{x_a}^{x_b} \left(-\left(B_0\right) \frac{d\varphi_j^{(2)}}{dx} \frac{d^2\varphi_i^{(1)}}{dx^2} \right) dx, \\
K_{jj}^{23} &= \int_{x_a}^{x_b} \left(\left(D_0 + G_0\right) \frac{d\varphi_j^{(2)}}{dx} \frac{d\varphi_j^{(2)}}{dx} \right) dx, & K_{jj}^{32} &= \int_{x_a}^{x_b} \left(\left(D_0 + G_0\right) \frac{d\varphi_j^{(2)}}{dx} \frac{d\varphi_j^{(2)}}{dx} \right) dx, \\
K_{jj}^{33} &= \int_{x_a}^{x_b} \left((A_0) \frac{d\varphi_j^{(2)}}{dx} \frac{d\varphi_j^{(2)}}{dx} \right) dx.
\end{aligned} \tag{17}$$

$$\begin{aligned}
\mathrm{M}_{ii}^{11} &= \int_{x_a}^{x_b} \left(\frac{\rho}{Q_{11}^k} C_0 \frac{d\varphi_i^{(1)}}{dx} \frac{d\varphi_i^{(1)}}{dx} + \rho b h \varphi_i^{(1)} \varphi_i^{(1)} \right) dx, & \mathrm{M}_{ij}^{12} &= \int_{x_a}^{x_b} \left(-\frac{\rho}{Q_{11}^k} \left(E_0 + H_0\right) \frac{d\varphi_i^{(1)}}{dx} \varphi_j^{(2)} \right) dx \\
M_{ji}^{21} &= \int_{x_a}^{x_b} \left(-\frac{\rho}{Q_{11}^k} \left(E_0 + H_0\right) \varphi_j^{(2)} \frac{d\varphi_i^{(1)}}{dx} \right) dx, & \mathrm{M}_{jj}^{22} &= \int_{x_a}^{x_b} \left(\frac{\rho}{Q_{11}^k} (F_0 + 2I_0 + J_0) \varphi_j^{(2)} \varphi_j^{(2)} \right) dx \\
\mathrm{M}_{ij}^{13} &= \int_{x_a}^{x_b} \left(-\left(\frac{\rho}{Q_{11}^k} B_0 \right) \frac{d\varphi_i^{(1)}}{dx} \varphi_j^{(2)} \right) dx, & \mathrm{M}_{ji}^{31} &= \int_{x_a}^{x_b} \left(-\left(\frac{\rho}{Q_{11}^k} B_0 \right) \frac{d\varphi_i^{(1)}}{dx} \varphi_j^{(2)} \right) dx, \\
\mathrm{M}_{jj}^{23} &= \int_{x_a}^{x_b} \left(\frac{\rho}{Q_{11}^k} \left(D_0 + G_0\right) \varphi_j^{(2)} \varphi_j^{(2)} \right) dx, & \mathrm{M}_{jj}^{32} &= \int_{x_a}^{x_b} \left(\frac{\rho}{Q_{11}^k} \left(D_0 + G_0\right) \varphi_j^{(2)} \varphi_j^{(2)} \right) dx, \\
M_{jj}^{33} &= \int_{x_a}^{x_b} \left(\left(\frac{\rho}{Q_{11}^k} A_0 \right) \varphi_j^{(2)} \varphi_j^{(2)} \right) dx
\end{aligned} \tag{18}$$

$$\begin{aligned}
& F_i^1 = \int_{x_a}^{x_b} \left(q \varphi_i^{(1)} \right) dx + Q_i, \; F_j^2 = Q_j, \; F_j^3 = Q_j, \\
& Q_1 \equiv -\widehat{V}_x\left(x_a\right), \; Q_2 \equiv -\widehat{M}_{xy}\left(x_a\right), \; Q_3 \equiv -\widehat{V}_x\left(x_b\right), \; Q_4 \equiv \widehat{M}_{xy}\left(x_b\right), \\
& Q_5 \equiv -\overline{M}_{xy}\left(x_a\right), \; Q_6 \equiv \overline{M}_{xy}\left(x_b\right), \; Q_7 \equiv -\widehat{N}\left(x_a\right), \; Q_8 \equiv \widehat{N}\left(x_b\right).
\end{aligned} \tag{19}$$

4 DISCUSSION OF NUMERICAL RESULTS

This section compares the efficiency of the Finite Element Method applied to ZZ theories (FEM-ZZ). For the static case, a comparison is made between the transverse and longitudinal displacement fields and the normal and shear stress fields for laminated composite beams subjected to sinusoidal loading. The number of layers (two, three and four) and the stacking configuration (0º/90º, 0/90º/0 e 0/90º/90º/0, see Figure 3), referring to the angle that the fibers form with the main axis of the beam, were considered in the response field analysis. The L/h ratio considered in these examples is 4, that is, a moderately thick beam where the effects due to shear make it prominent over those of flexion. In these analyzes, the results obtained by FEM-ZZ are compared with the analytics developed by Pagano [14]. For dynamic analysis, it is considered the same beam of Figure 3 subjected to free vibration. In this dynamic consideration, the beam has the stacking configuration equal to 0º/90º e 0º/90º/0º and the L/h ratio varying in 100, 10 and 5. The results obtained by FEM-ZZ are compared to those obtained by the three-dimensional FEM. shown in Giunta et al. [15]. In all the examples is considered the graphite-epoxy material whose Young modulus and Poisson ratio are:

$$E_x = 25\ MPa \qquad G_{xy} = 0.5\ MPa$$
$$E_y = 1\ MPa \qquad G_{yz} = 0.2\ MPa$$
$$v_{xy} = v_{yz} = 0.25$$

a)

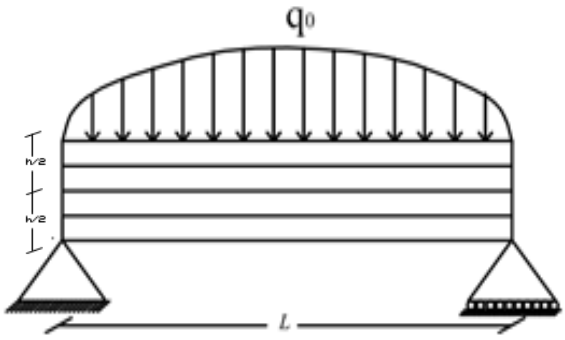

b)

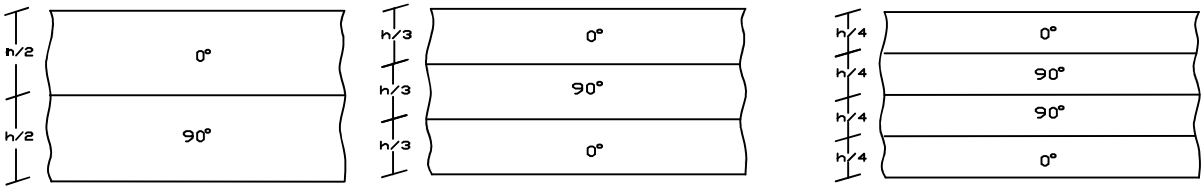

Figure 2 a) Simply supported beam subjected to a sinusoidal load; b) Fibers arrangements in laminated beams.

For the results to be independent of the geometric and loading parameters, the response fields were dimensionless as follows:

$$\overline{u}\left(0,z,0\right) = \frac{uE_y b}{q_0 h}, \quad \overline{w}\left(x,0\right) = \frac{100wE_y bh^3}{q_0 L^4}, \quad \overline{\sigma}_{xx}\left(\frac{L}{2},z,0\right) = \frac{b\sigma_{xx}}{q_0},$$
$$\overline{\tau}_{xz}\left(0,z,0\right) = \frac{b\tau_{xz}}{q_0}, \quad \overline{\omega} = \omega\left(L^2\sqrt{\frac{\rho bh}{A_0}}\right), \quad S = \frac{L}{h}, \tag{20}$$

where $\overline{u}$ is the dimensionless longitudinal displacement of the cross section, $\overline{w}$ is the dimensionless deflection in the middle of the beam, $\overline{\sigma}_{xx}$ is the dimensionless normal stress, $\overline{\tau}_{xz}$ is the dimensionless

shear stress, q_0 is the amplitude of the sinusoidal load and $\bar{\omega}$ is the natural frequency of the first mode of vibration. The L2-Norm error was calculated by the expression:

$$\text{relative error}_{L2}(\%) = \frac{\sqrt{(VR_1 - VC_1)^2 + (VR_2 - VC_2)^2 + \ldots + (VR_n - VC_n)^2}}{\sqrt{(VR_1)^2 + (VR_2)^2 + \ldots + (VR_n)^2}} \times 100\% . \qquad (21)$$

where VR_i e VC_i $(i = 1,2 \ldots n)$ are calculated reference values, respectively.

4.1 Static Analysis

4.1.1 Two cross-ply laminated beam under transverse loading [0º/90º]

Figure 3(a - d) shows the results for the displacement and stress fields when various kinematics are used in the FEM-ZZ (16-element). The deflection, w, was aproximated by Hermite cubic polynomials. The axial displacement u_o and rotation ϕ were approximated by Lagrange quadratic polynomials.

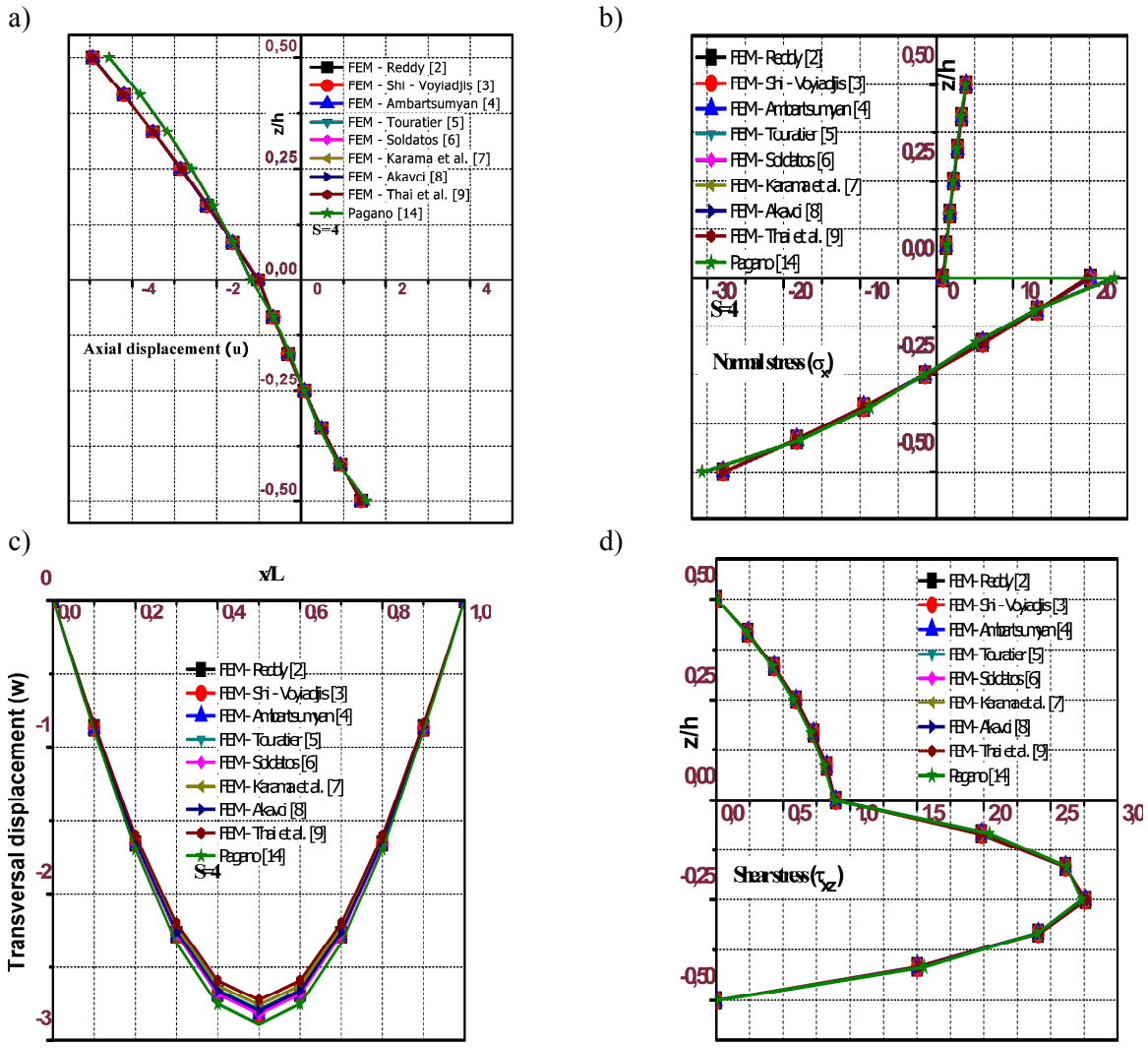

Figure 3. Field of (a) axial displacement, (b) normal stress, (c) transverse deflection along the beam, (d) shear stress when using 16-element FEM-ZZ. Response fields (a) and (d) are related to *x* = *L* and fields (b) and (c) are related to *x* = *L/2* to the beam [0º/90º].

Figures 4(a - d) show the L2-Norm errors between the various kinematics used and the reference solution (Pagano [14]) as the number of elements is increased. Figure 3 shows the good agreement of the results obtained by the various FEM-ZZ kinematics in relation to the reference solution. Figure 4 shows the convergence of results after the use of 16 elements. Analyzing Figs. 3 and 4 shows the low influence of high order theories on the mechanical effects of the beam. Overall, all theories performed similarly with errors less than 10%, 9.5%, 4%, and 2% for the effects of axial displacement, normal stress, transverse deflection, and shear stress, respectively.

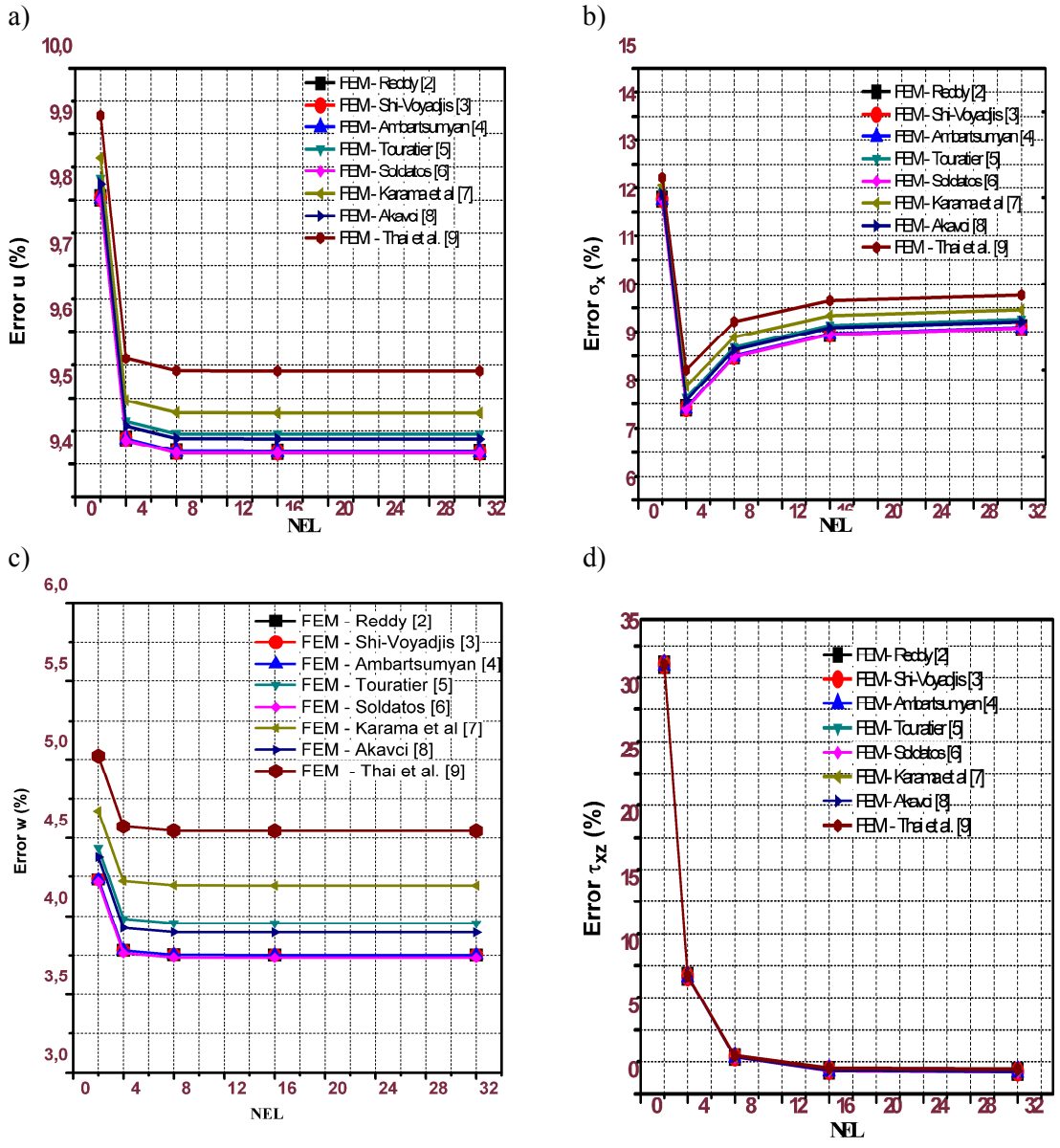

Figure 4. L2-Norm errors: a) axial displacement, b) normal stress, c) transverse deflection and d) shear stress as the number of elements (NEL) increases. The response fields (a) and (d) are related to $x = L$ and fields (b) and (c) are related to $x = L/2$ to the beam [0º/90º].

4.1.2 Three cross-ply laminated beam under transverse loading [0°/90°/0°]

For this example, the main advantages of the ZZ theory were highlighted. The approximation used to obtain the solutions showed in Figs. 5 (a-d) is again Hermite's cubic, for w, and Lagrange's quadratic for axial displacement u_o and rotation ϕ , with 16 elements. It is observed in Fig. 5a the zigzag behavior of the ZZ theory obtaining an error of less than 14% when considering the parabolic theories. The axial tension is presented in Fig. 5b, with greater emphasis on the parabolic Soldatos theories [6], with errors less than 12%. The transverse displacement and shear stress are presented in Figs. 5c and 5d, both obtained errors less than 5% when considering the parabolics and Soldatos theories [6]. Among the studied theories, Thai et al. [9] obtained the lowest efficiency.

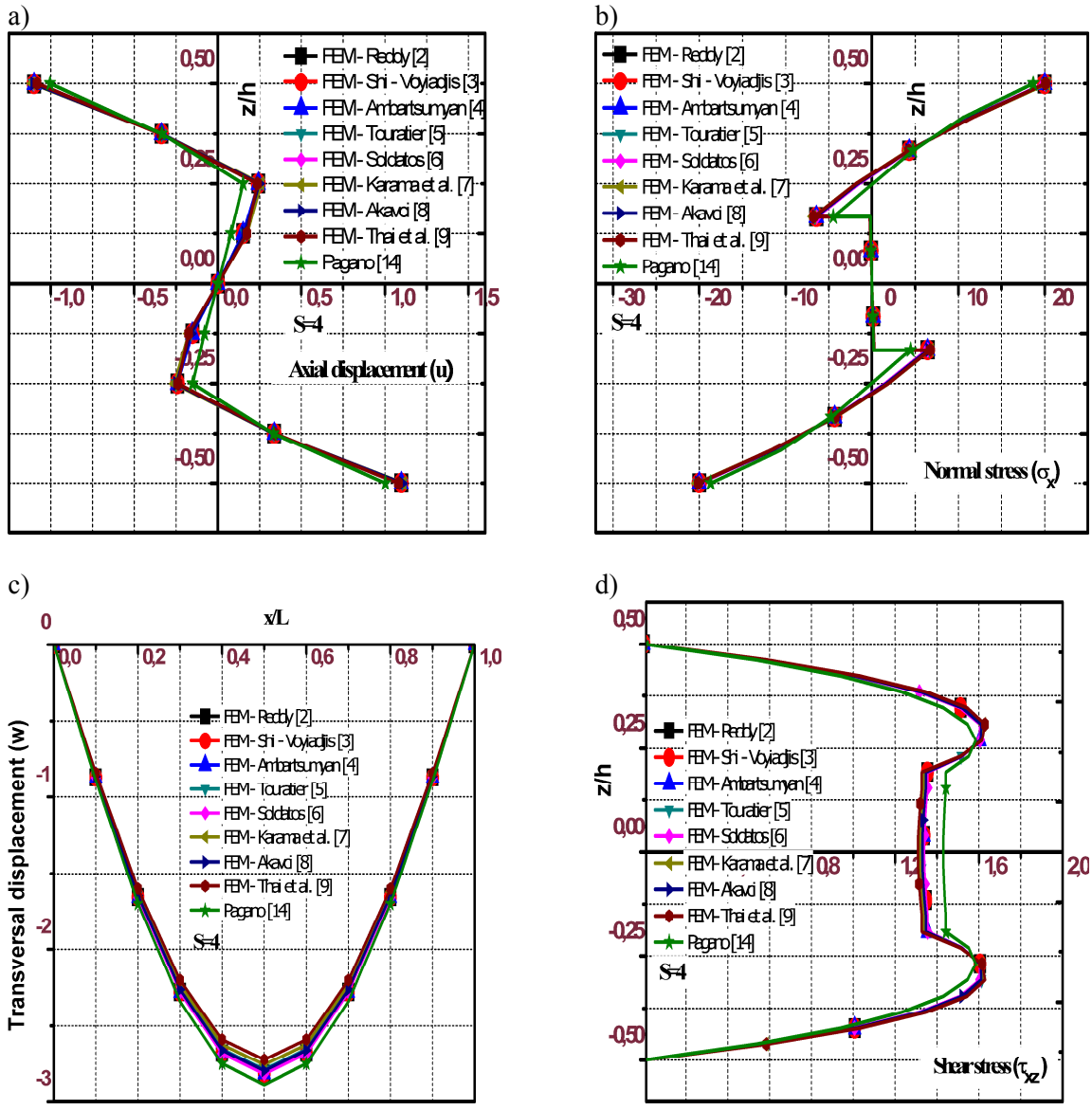

Figure 5. Beam behavior: (a) axial displacement, (b) normal stress, (c) transverse deflection along the beam, (d) shear stress when using 16-element FEM-ZZ. Response fields (a) and (d) are related to $x = L$ and fields (b) and (c) are related to $x = L/2$ to the beam [0°/90°/0°].

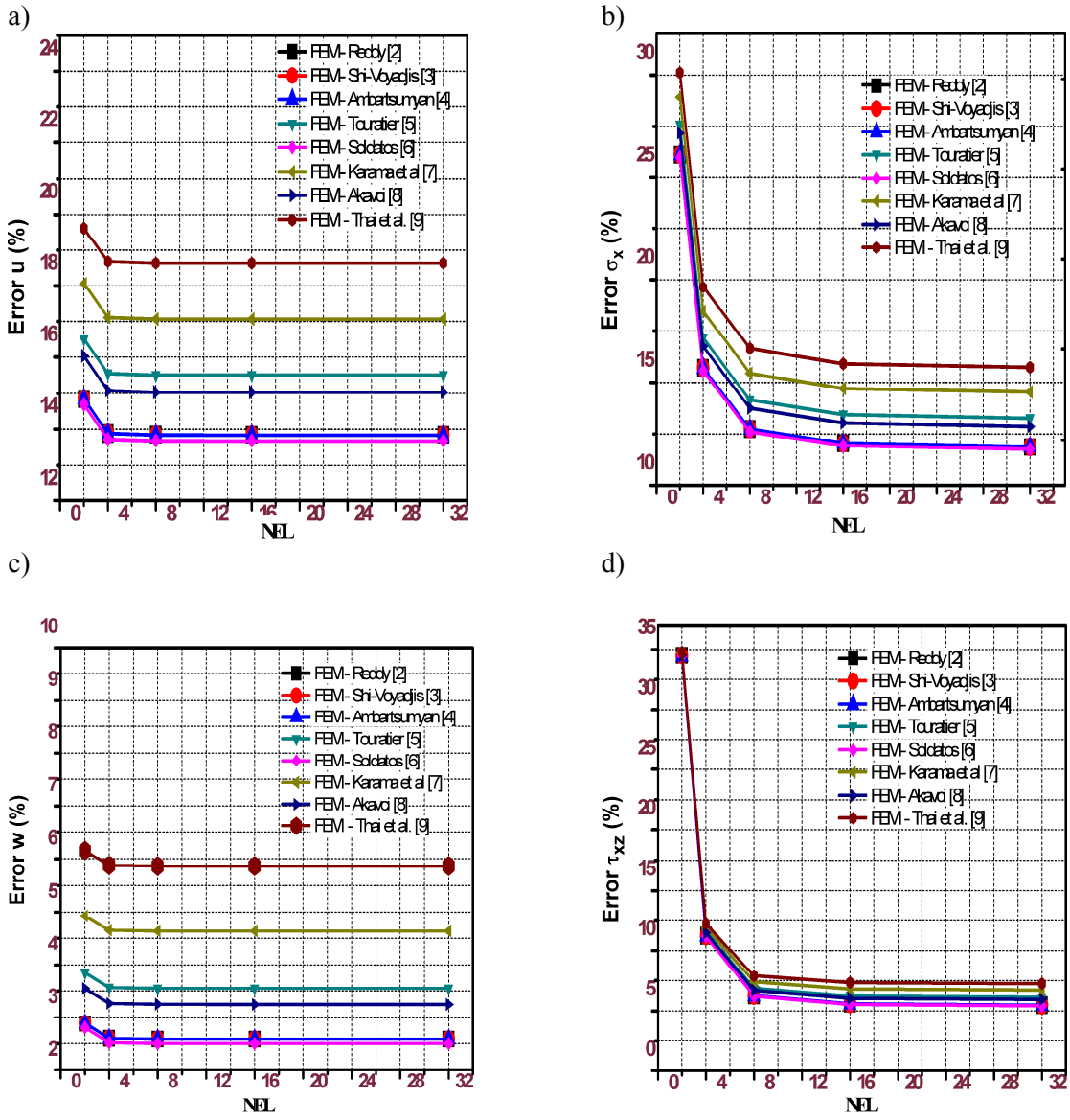

Figure 6. L2-Norma errors: a) axial displacement, b) normal stress, c) transverse deflection and d) shear stress as the number of elements (NEL) increases. Response fields (a) and (d) are related to x = L and fields (b) and (c) are related to *x = L/2* to the beam [0º/90º/0º].

4.1.3 Four cross-ply laminated beam under transverse loading [0º/90º/90º/0º]

For this example was used, again 16 elements and the same approximated polynomials of the previous example. From the results presented in Figs. 7 (a-d) it is possible to observe again the good efficiency of the ZZ theory. The parabolic theories and trigonometric theories of Soldatos [6] obtained the best results in relation to the others. The smallest errors obtained for these theories were 11%, 8%, 1.5% and 1.5% for axial displacement, normal stress, transverse deflection and shear stress, respectively. Figure 8 show the convergence of FEM-ZZ from 16 elements.

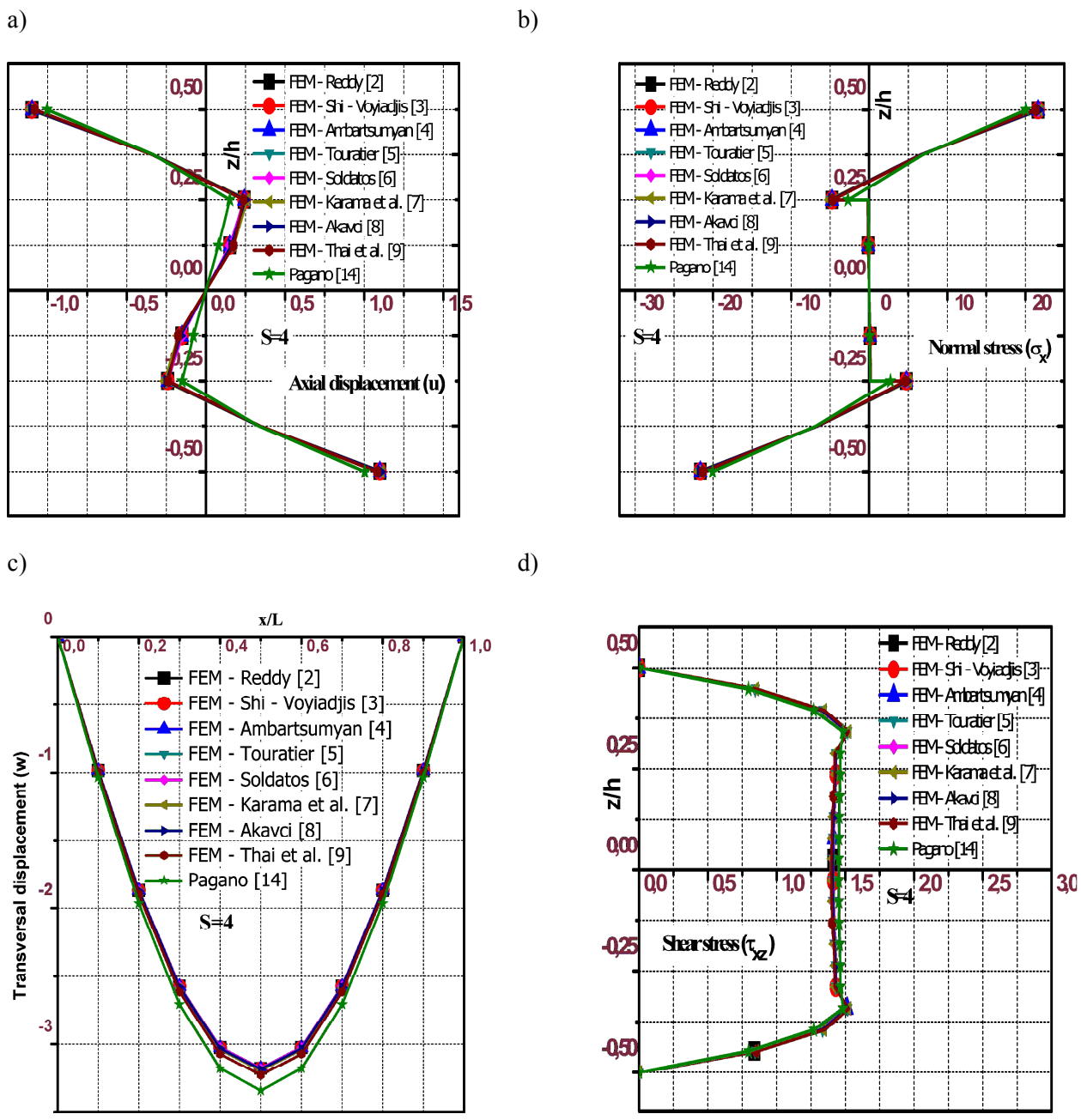

Figure 7. Fields of: (a) axial displacement, (b) axial stress, (c) transverse deflection along the beam, (d) shear stress when using 16-element FEM-ZZ. Response fields (a) and (d) are related to $x = L$ and fields (b) and (c) são related to $x = L/2$ to the beam [0°/90°/90°/0°].

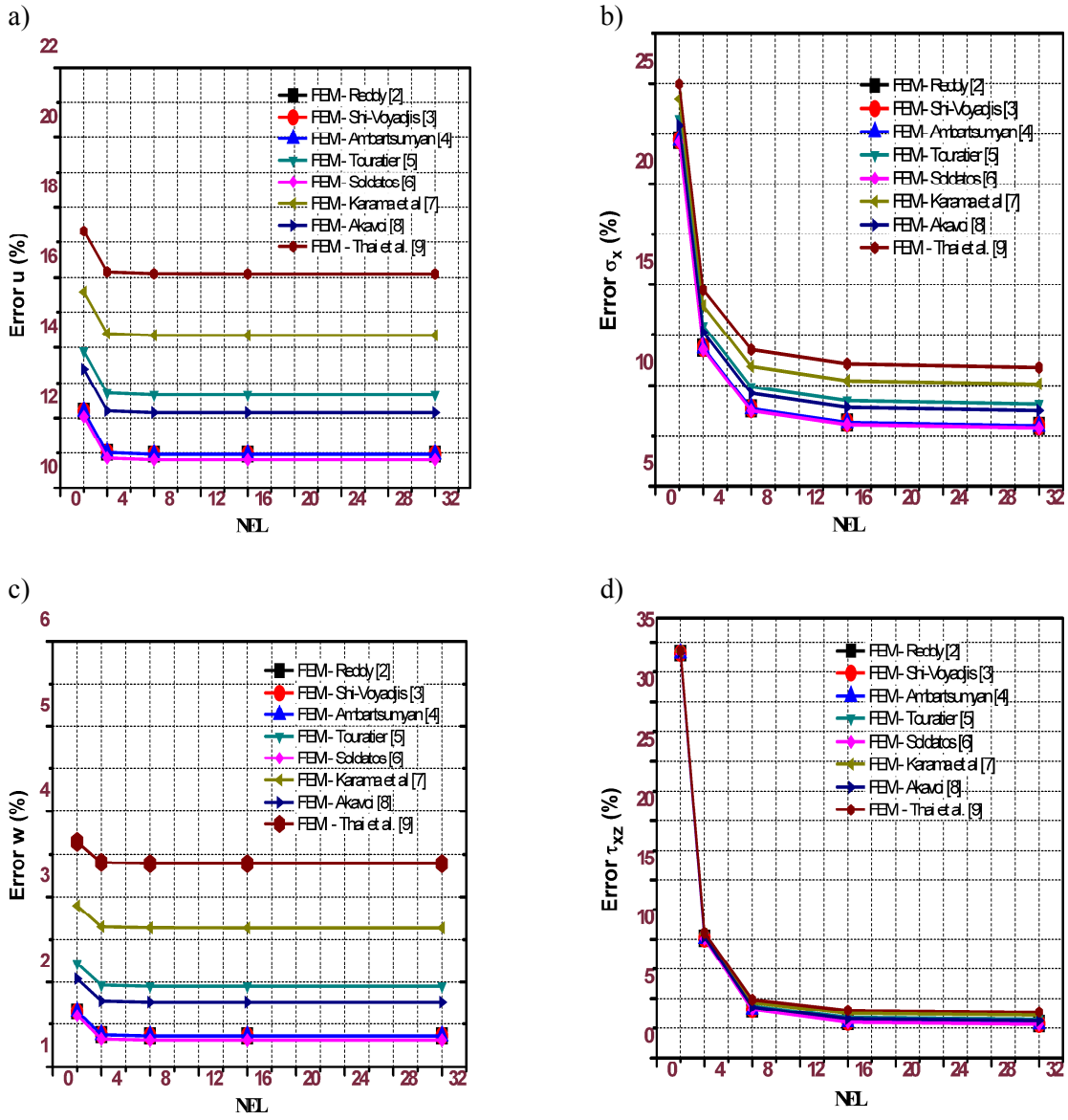

Figure 8. L2-Norm errors: a) axial displacement, b) axial stress, c) transverse deflection and d) shear stress as the number of elements (NEL) increases. The response fields (a) and (d) are related to $x = L$ and fields (b) and (c) are related to $x = L/2$ for the beam [0°/90°/90°/0°].

4.1.4 Shear Locking

The shear locking effect corresponds to not recovering the correct response field as the beam becomes thin. To show the absence of this effect, the maximum transverse displacement of a beam [0º/90º/0º] using FEM – ZZ (16 elements) is shown in Fig. 9, as the *L/h (S)* ratio increases. In addition to the theories developed here, we also show the Euler-Bernoulli (EBT) theory which has a field of response independent of the value of S. It is evident that all theories seek to recover the analytical value developed by Pagano [14] for both, moderately thick and thin beams.

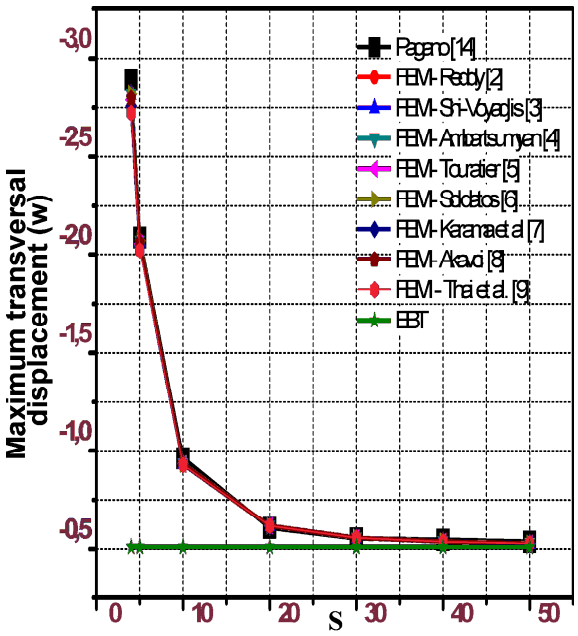

Figure 9. Maximum transverse displacement $\overline{w}$ of the beam as L/h(S) ratio increases [0º/90º/0º].

4.2 Free vibration analysis

The natural frequency is obtained by solving the eigenvalue problem proposed in Eqs. (23), using the Finite Element Method. Thus, the approximation for the vibration modes $W(x)$ and $S(x)$ are shown in Eq. (22):

$$W(x) \approx \sum_{i=1}^{m} W_i \varphi_i^{(1)}(x), \quad U(x) \approx \sum_{j=1}^{n} U_j(t) \varphi_j^{(2)}(x), \quad S(x) \approx \sum_{j=1}^{n} S_j(t) \varphi_j^{(2)}(x), \tag{22}$$

where $\varphi_j^{(1)}$ and $\varphi_j^{(2)}$ are Hermite cubic and Lagrange quadratic polynomial interpolation functions, respectively. The finite element model is given by:

$$\begin{bmatrix} [K^{11}] & [K^{12}] & [K^{13}] \\ [K^{21}] & [K^{22}] & [K^{23}] \\ [K^{31}] & [K^{32}] & [K^{33}] \end{bmatrix} - \omega^2 \begin{bmatrix} [M^{11}] & [M^{12}] & [M^{13}] \\ [M^{21}] & [M^{22}] & [M^{23}] \\ [M^{31}] & [M^{32}] & [M^{33}] \end{bmatrix} \begin{Bmatrix} \{W\} \\ \{S\} \\ \{U\} \end{Bmatrix} = \begin{Bmatrix} \{0\} \\ \{0\} \\ \{0\} \end{Bmatrix}. \tag{23}$$

To show the efficiency of the model proposed in Eq. (23) is considered a simply supported beam subject to free vibration. The stacking configurations used were [0º/90º] and [0º/90º/0º] and its L/h ratio varied in 100, 10 and 5. It was observed the convergence of the model using 8 elements. Tables 2 and 3 compare the FEM-ZZ (8 elements) and the three-dimensional FEM solution shown in Giunta et al. [15].

The natural frequency obtained was dimensionless according to Eq. (20). It is evident that all theories have a good efficiency in obtaining the natural frequency with relative errors less than 1%. Among the presented theories, the parabolic ones had the highest efficiency, with a maximum error of 0.7% for all analyzed cases. Also noteworthy is the efficiency of FEM – ZZ for both thin and moderately thick beams.

Table 2. Natural frequency $\overline{\omega}$ for a simply supported beam [0º/90º/0º].

Author	S = 100	S = 10	S = 5
Reddy [2]	13,948	10,345	6,940
Shi-Voyiadjis [3]	13,948	10,345	6,940
Ambartsumyan [4]	13,948	10,345	6,940
Touratier [5]	13,948	10,352	6,962
Soldatos [6]	13,948	10,344	6,938
Karama et al. [7]	13,948	10,364	6,989
Akavci [8]	13,948	10,350	6,955
Thai et al. [9]	13,948	10,380	7,022
FEM 3D [13]	13,932	10,334	6,888

Table 3. Natural frequency $\overline{\omega}$ for a simply supported beam [0º/90º].

Author	S = 100	S = 10	S = 5
Reddy [2]	6,175	5,807	5,016
Shi-Voyiadjis [3]	6,175	5,807	5,016
Ambartsumyan [4]	6,175	5,807	5,016
Touratier [5]	6,175	5,808	5,019
Soldatos [6]	6,175	5,807	5,015
Karama et al. [7]	6,175	5,810	5,024
Akavci [8]	6,175	5,808	5,018
Thai et al. [9]	6,175	5,812	5,030
FEM 3D [13]	6,169	5,772	4,936

5 CONCLUSIONS

In this paper, a finite element model was developed for several high-order Zig-Zag theories. All theories were observed to have a similar performance, especially the parabolic theories - which had the same performance - and the trigonometric theory of Soldatos [6]. ZZ theories showed good efficiency for both, static and dynamic effects. In particular, the effects of transverse displacement, shear stress and free vibration showed errors less than 5% in all analyzed examples. In general, FEM – ZZ presented convergence without shear locking effect using from 16 elements.

Acknowledgements

The authors would like to acknowledge Federal University of Sergipe (PIBIC/COPES), Coordenação de Aperfeiçoamento de Pessoal de Nível Superior – Brazil (CAPES) – Finance code 001 for the financial support.

References

[1] Timoshenko S.P.. *On the correction for shear of the differential equation for transverse vibrations of prismatic bars*, Philosophical Magazine 41, 744-746, 1921
[2] J.N. Reddy. *A simple higher-order theory for laminated composite plates.* Journal of Applied

Mechanics, v. 51, n. 4, p. 75–752, 1984.
[3] G. Shi and G.Z. Voyiadjis. *A Sixth-Order Theory of Shear Deformable Beams With Variational Consistent Boundary Conditions*. Journal of Applied Mechanics, v. 78, n. 2, p. 21019, 2011.
[4] S.A. Ambartsumyan. *On theory of bending plates*. Izv Otd Tech Nauk AN SSSR, v. 5, n. 5, p. 69–77, 1958.
[5] M. Touratier, An efficient standard plate theory, Int. J. Eng. Sci., vol. 29, no. 8, pp. 901–916, 1991.
[6] K.P. Soldatos, *A transverse shear deformation theory for homogeneous monoclinic plates*, Acta Mechanica, vol. 94, pp. 195–200, 1992.
[7] M. Karama , K. S. Afaq and S. Mistou*, Mechanical behavior of laminated composite beam by new multi-layered laminated composite structures model with transverse shear stress continuity*, Int. J. Solids Struct., vol. 40, no. 6, pp. 1525–1546, 2003.
[8] S. S. Akavci, *Buckling and free vibration analysis of symmetric and anti-symmetric laminated composite plates on an elastic foundation*, J. Reinf. Plast. Compos., vol. 26, no. 18, pp. 1907–1919, 2007.
[9] C. H. Thai, A. J. Ferreira, S.P. Bordas,T. Rabczuk and H. Nguyen-Xuan . *Isogeometric analysis of laminated composite and sandwich plates using a new inverse trigonometric shear deformation theory. Eur J Mech* – A Solids;43:89–108, 2014.
[10] A. S. Sayyad, Y. M. Ghugal and R. R. Borkar . *Flexural analysis of fibrous composite beams under various mechanical loadings using refined shear deformation theories.* Composites: Mechanics, Computations, Applications. An International Journal 5(1), 1–19, 2014.
[11]J. N. Reddy. *Mechanics of laminated composite plates and shells. Theory and analysis*. Boca Raton: CRC Press; 2004.
[12] M. DiSciuva. *Multilayered anisotropic plate models with continuous interlaminar stresses*. Compos Struct;22(3):149–167, 1992.
[13] M. DiSciuva, M. Gherlone, L. Lurlaro and A. Tessler. *A class of higher-order C0 composite and sandwich beam elements based on the Refined Zigzag Theory*. Compos Struct. 132 784–803, 2015.
[14] N. J. Pagano. *Exact solution for composite laminates in cylindrical bending*. J Compos Mater 1969;3:398–411.
[15] G. Giunta, F. Biscani, S. Belouettar, et al. *Free vibration analysis of composite beams via refined theories*. Compos: Part B; 44: 540–552, 2013.
[16] J. N. Reddy. *Energy and Variational Methods in Applied Mechanics*.. New York: John Wiley, 1984.